Hydrol. Earth Syst. Sci. Discuss., doi:10.5194/hess-2016-1, 2016
Manuscript under review for journal Hydrol. Earth Syst. Sci.
Published: 19 January 2016

Hydrology and Earth System Sciences
Discussions

A post-wildfire response in cave dripwater chemistry

Gurinder Nagra[1*], Pauline C. Treble[1, 2], Martin S. Andersen[1], Ian J. Fairchild[3], Katie Coleborn[1], Andy Baker[1]

[1] {Connected Waters Initiative Research Centre, University of New South Wales, Sydney, NSW, 2052, Australia}

[2] {Institute for Environmental Research, Australian Nuclear Science and Technological Organisation, Lucas Heights, NSW, 2234, Australia}

[3] {School of Geography, Earth and Environmental Sciences, University of Birmingham, Edgbaston, Birmingham, UK}

Correspondence to: G. Nagra (g.nagra@unsw.edu.au)

Hydrol. Earth Syst. Sci. Discuss., doi:10.5194/hess-2016-1, 2016
Manuscript under review for journal Hydrol. Earth Syst. Sci.
Published: 19 January 2016

Hydrology and Earth System Sciences
Open Access
Discussions

Abstract

Cave environments are sensitive because surface environmental changes can affect both the isotopic composition and solute concentration of infiltrating cave dripwaters. These changes subsequently affect the speleothem geochemical record. One such agent of change is wildfire, however its effect on karst processes remains poorly understood. Using dripwater data from a shallow cave, at a forested site in southwest Australia, we provide a unique analysis of the post-wildfire effects on dripwater $\delta^{18}O$ and solute concentrations. We analyse how wildfires affect on local controls, i.e. vegetation cover, evapotranspiration and carbonate water-rock interactions, effects cave dripwater hydrology and geochemistry. We compare our post-wildfire data with modelled drip water $\delta^{18}O$, regional groundwater chemistry, and a second cave dripwater dataset, to determine the extent to which wildfire affects cave dripwater composition. We find in our forested, shallow cave site, by effecting surface evaporation and transpiration rates wildfire can have a multi-year impact on subsurface hydrology and dripwater chemistry. Here we open a new avenue for speleothem science in fire-prone regions, focusing on the geochemical records of speleothems as potential paleo-fire archives.

Hydrol. Earth Syst. Sci. Discuss., doi:10.5194/hess-2016-1, 2016
Manuscript under review for journal Hydrol. Earth Syst. Sci.
Published: 19 January 2016

Hydrology and Earth System Sciences
Discussions

1 Introduction

Caves are observatories that contain invaluable geochemical archives of past-climates; preserved in the form of speleothems (stalagmites, stalactites and flowstones). The existing paradigm in speleothem science has largely focused on establishing paleoclimate proxies in stalagmites (McDermott et al., 2001; Treble et al., 2008; Woodhead et al., 2010). While these proxies have been useful for reconstructing paleoclimates, their interpretations may hold a predisposed bias towards using these proxies as indicators of paleo-climates only, instead of including local environmental factors.

One way of verifying these paleoclimate proxies has been to conduct dripwater monitoring studies. To date dripwater monitoring has predominantly focused on understanding the extent to which climatic controls affect dripwater $\delta^{18}O$ (Lachniet, 2009) and solute concentration (Fairchild and Treble, 2009). Further, such studies have largely been restricted to mid to high latitude climate regions where precipitation is larger than evapotranspiration (P > AET). However, the exception – studies in water-limited regions – tell a different story. Here dripwater chemistry is influenced to a greater extent by environmental factors such as evaporation (Pape et al., 2010; Cuthbert et al., 2014; Rutlidge et al., 2014) and transpiration (Tremaine and Froelich, 2013; Treble et al., submitted).

While evaporation and transpiration are climate induced, wildfires – common in water-limited regions - are an agent of change than can dramatically alter evaporation and transpiration rates by destroying vegetation. The potential impacts of vegetation loss due to fire are both short-term and long-term. The short-term impacts include: (1) an increase in evaporation rates due to changes in albedo and/or lack of shading (Silberstein et al., 2008); (2) a reduction in transpiration; (3) a reduction in soil microbial and root CO_2 production (Coleborn et al., 2016); (4) a decrease in-cave air CO_2 which can influence Mg/Ca and Sr/Ca compositions (Wong and

Hydrol. Earth Syst. Sci. Discuss., doi:10.5194/hess-2016-1, 2016
Manuscript under review for journal Hydrol. Earth Syst. Sci.
Published: 19 January 2016

63 Banner, 2010); (5) the addition of plant ash to the soil profile, increasing concentrations of Ca,
64 K, Mg and S (Grove et al., 1986; Yusiharni and Gilkes, 2012a); and (6) altered infiltration
65 patterns (González-Pelayo et al., 2010). Long-term impacts include: (1) the spatial
66 redistribution of nutrients (Abbott and Burrows, 2003); (2) regrowth impacts on water balance
67 and nutrient flux (Treble et al., submitted); and (3) a reduction in total soil CO_2 due to the
68 destruction of CO_2 sequestering microbial communities and plant roots, both significant
69 sources of soil CO_2 (Coleborn et al., 2016). Despite wildfires regularly impacting water-limited
70 regions, its impact on $\delta^{18}O$ and solute concentrations in cave dripwater has not been reported.

71 Here, we analyse dripwater compositions from five years of drip monitoring (August 2005 -
72 March 2011) in a shallow cave system in southwest Australia following an intense wildfire in
73 February 2005. We compare this dripwater data to the regional groundwater geochemistry and
74 published cave dripwater from another cave in the southwest Australia (Treble et al. 2015).
75 Our analysis provides a unique analysis of the impact of wildfire on (1) cave dripwater,
76 challenging the existing use of $\delta^{18}O$ and solute concentrations for paleoclimate proxies in
77 water-limited regions; (2) local water balance and; (3) bioproductivity during the initial post-
78 fire period, in which vegetation is removed, as well as during the subsequent period of forest
79 regeneration.

80

81 ## 2 Site description

82 Our study was conducted in Yonderup Cave in Yanchep National Park (lat 31.5475 S, long
83 115.690833 E), 20 km north of Perth, southwestern Australia (Fig. 1A). This region has a
84 Mediterranean climate characterised by dry hot summers and colder wet winters with an
85 average yearly surface temperature of 15.1 ^{o}C and a 25 year average annual rainfall of 664 mm
86 with 85% falling between May and October. Yonderup cave is located in the Tamala Limestone

Hydrol. Earth Syst. Sci. Discuss., doi:10.5194/hess-2016-1, 2016
Manuscript under review for journal Hydrol. Earth Syst. Sci.
Published: 19 January 2016

Hydrology and Earth System Sciences
Discussions

Formation, a porous, partially lithified calcareous coastal dune sand. This karst process is said to be "syngenetic" with karstification occurring simultaneously with lithification of the host rock (Jennings, 1964; Fairchild and Baker, 2012).

Yonderup Cave is situated in a tuart forest *(Eucalyptus gomphocephala)*, with mature tuart trees 30 m high, and an understory of shrubs and trees standing 5-10 m high, Sheoak trees (*Allocasuarina fraseriana)* approx. 5-15 m high, and Balga trees (*Banksia attenuata*, *Banksia menziesii*, *Banksia grandis*, *Allocasuarina fraseriana*, *Xanthorrhoea pressii*). Tree roots are exposed in the cave, both in the roof (fine roots), and cave floor (thick tap roots). In February 2005, the area above the cave was burnt in an intense wildfire (Fig. 1B, Department of Parks and Wildlife, pers. comm., 2015), substantially modifying vegetation above the cave including death of mature trees and complete removal of canopy and understorey in some areas.

Over the period of August 2005 to March 2011, two drip sites in Yonderup Cave (Site 1a and Site 2a), were monitored for their chemical and hydrological variations. These two sites are 22.8 m apart (Site 2a east of Site 1a, ~ 1 m slope towards the East), located at similar depths below the surface (~ 4 m) within the same chamber (~ 7 m height) and partially separated by a large boulder fall-in. We use an existing cave survey to determine the location of each cave drip site relative to the ground surface (Fig. 1). We also compare Mg/Ca and Sr/Ca concentrations between drip sites to make sure each drip has an independent flow path (Fig. 2). A soil depth survey was conducted within 5 m of each site (Sup. Table 4), along with visual vegetation/ground surface observations post-fire. Soil depths were measured every meter with a dynamic soil penetrometer in north, south, east and west directions and averaged soil depth above each site were calculated.

Site 1a, 30 m from the cave entrance, has a drip source within a large cluster of soda-straw stalactites known as the 'Wheatfield' (Sup. Figure 2B). This circular feature is approximately

Hydrol. Earth Syst. Sci. Discuss., doi:10.5194/hess-2016-1, 2016
Manuscript under review for journal Hydrol. Earth Syst. Sci.
Published: 19 January 2016

1 m across and as it appears in an otherwise very sparsely decorated part of the ceiling, suggests that it represents a focused flow path into the cave. The land surface above this site is flat with 70% covered by shallow heterogeneous soil (average 124 mm thickness) and the remaining surface is bedrock exposure (approx. 30%). A dead tuart tree, killed and collapsed during the 2005 wildfire, lies directly above Site 1a, entirely removing the upper canopy directly above Site 1a as no other canopy trees are close enough to provide canopy cover.

In contrast, Site 2a situated 50 m from the cave entrance is in a highly decorated part of the cave known as the 'Cathedral' characterised by large icicle shaped stalactites. Above Site 2a, the soil cover is thicker (200 mm) and more homogenous with no bedrock exposure, and no trees directly above, however there is a partial canopy cover from adjacent trees ~15 m away.

3 Data collection

Cave dripwater was collected from 1L high-density polyethylene (HDPE) collection vessels at the two sites Site 1a and Site 2a between August 2005 and March 2011 at approximately bi-monthly intervals. The water was separated into three aliquots: two aliquots were filtered with 0.45 µm mixed-cellulose filters into two 50 ml polypropylene bottles for major and minor ion determination; the third was stored with zero-headspace in a 12 ml amber glass bottle for stable isotopes. All aliquots were refrigerated below 5°C until analysis. Anion concentrations (Cl and SO_4) were determined using a Dionex DX-600 ion chromatograph with self-regenerating suppressor on one aliquot. The second aliquot was acidified to 2% HNO_3 in the collection bottle and used for cation concentrations (Ca, K, Mg, Na, Si and Sr) using a Thermo Fisher inductively coupled plasma-atomic emission spectroscopy (ICP-AES) ICAP7600. An internal standard with concentrations approximating the cave waters was included in each cation batch to check for between-run reproducibility.

Hydrol. Earth Syst. Sci. Discuss., doi:10.5194/hess-2016-1, 2016
Manuscript under review for journal Hydrol. Earth Syst. Sci.
Published: 19 January 2016

Dripwaters collected between August 2005 and May 2008 were analysed for $\delta^{18}O$ using Isotope-Ratio Mass Spectrometry (IRMS) at the Australian National University (see Treble et al., 2013 for method). The remaining dripwaters were analysed for $\delta^{18}O$ and $\delta^{2}H$ at ANSTO using the Cavity Ring Down Spectroscopy (CRDS) method. Additionally, as there was sufficient remaining water in the stored aliquots analysed by IRMS for Site 2a, these were also re-analysed using CDRS to obtain a complete time series for $\delta^{2}H$. After Jan 2007 dripwater volume at Site 1a became insufficient to collect all three aliquots. Collections of aliquots were prioritised in the following order: 1) stable isotopes; 2) cations and; 3) anions.

At each cave visit for dripwater sampling, drip rates were manually recorded using a stopwatch and the level of water accumulated in the bottles was recorded to the nearest 100 ml. Weekly discharge was estimated using a drip volume of 0.2 ml per drip (Collister and Mattey, 2008). When timing drip intervals became impractical, only the bottle level was recorded. The period of overlapping measurements by the two drip recording methods was used to calculate weekly discharge based on the bottle volume recordings for the periods where the stopwatch method could not be used.

To distinguish dry and wet periods we applied a residual mass curve (RMC), (Hurst, 1951) to monthly P - AET data. This is the cumulative sum of the monthly anomaly calculated from the 22 year mean and used to generate a time series of cumulative potential water surplus or deficit starting from Jan 2000, highlighting trends in above average or below average P – AET, we refer to this calculation as cumulative water balance (CWB) throughout the rest of this paper.

Unpublished monthly $\delta^{18}O$ and $\delta^{2}H$ rainfall data (2005 – 2011) from Perth were obtained from the Australian Nuclear Science and Technology Organisation (ANSTO; unpublished). Modelled regional precipitation (P) and actual evapotranspiration (AET or FEW is the sum of soil evaporation and transpiration by vegetation based on Priestly-Taylor equations) from the

Hydrol. Earth Syst. Sci. Discuss., doi:10.5194/hess-2016-1, 2016
Manuscript under review for journal Hydrol. Earth Syst. Sci.
Published: 19 January 2016

159 Australian Water Availability Project (AWAP) (Raupach et al., 2009; Raupach et al., 2011)
160 were used with monthly parameters, to determine P – AET. AWAP precipitation (P), actual
161 evapotranspiration (AET) and rainfall $\delta^{18}O$ data was then used as input data in a forward model
162 (detailed in the next section) to predict cave dripwater $\delta^{18}O$ composition. Predictions are based
163 solely on P - AET data which are then compared to the dripwater observations.

164 Monthly rainfall $\delta^{18}O$ and $\delta^{2}H$ compositions were amount weighted and fitted with a linear
165 regression (Hughes and Crawford, 2012) and compared to the long-term groundwater mean
166 obtained from Turner and Thorpe (2001) and the cave drip data to determine whether
167 evaporation has affected cave dripwater isotopic composition (see section 4).

168 Post-fire solute and $\delta^{18}O$ data from Yonderup dripwater are also compared to other relevant
169 published data. These include, long term Perth rainfall $\delta^{18}O$ from Turner and Thorpe and Cook
170 (2001), and local Yanchep rainfall solute data from Hingston and Gailitis, (1976), and
171 published dripwater data from Golgotha Cave, located 300 km south of Yanchep. Golgotha
172 Cave has been monitored since 2005 (Treble et al., 2013; Treble et al., 2015; Treble et al.,
173 submitted; Mahmud et al., 2015). The climate at Golgotha Cave is also Mediterranean, but
174 receives rainfall of approx. 795 mm/a, which is 23% higher than Yanchep. Both caves are
175 located within the Tamala Limestone Formation, however the caves vary in depths: Golgotha
176 Cave is significantly deeper than Yonderup approx. 30 - 35 m. Golgotha Cave is covered by a
177 more extensive forest of mixed marri/karri (*Eucalyptus calophylla / Eucalyptus diversicolor*)
178 trees and this site has not experienced an intense wildfire since 1992 and no prescribed burns
179 since 2006.

180

Hydrol. Earth Syst. Sci. Discuss., doi:10.5194/hess-2016-1, 2016
Manuscript under review for journal Hydrol. Earth Syst. Sci.
Published: 19 January 2016

Hydrology and Earth System Sciences
Open Access
Discussions

4 Forward model

To compare our measured post-fire dripwater $\delta^{18}O$ to the values expected in the case where there is no fire, we forward model dripwater $\delta^{18}O$ based on a monthly discretised water balance and a mass balance for $\delta^{18}O$ using the same method as Baker et al., (2010). The model permits the mixing of the isotopic composition of incoming monthly rainwater in the soil and epikarst where inputs are governed by monthly rainfall isotopic composition and rainfall amount, and outputs by monthly AET and infiltration into a seepage reservoir and into fracture-fed flow. The latter are determined by hydrological thresholds (see Baker and Bradley, 2010). This appropriately reflects our knowledge of the geology of the Tamala Limestone, which retains a high primary porosity (the seepage reservoir) whilst fractures focus flow to specific regions of the cave ceiling (Treble et al., 2013; Mahmud et al., in review).

Water entering the seepage reservoir has a storage time that is expressed as a Gaussian distribution. This is prescribed with a maximum age of 3 years, reflecting the shallow depth of our cave system, and a mean and standard deviation that can be specified. In contrast, the fracture-fed flow is instantaneously passed through the system (i.e. with a travel time of less than one month). Thresholds for water movement to the seepage reservoir and fracture flow can be specified to reflect the observed variability of dripwater discharge. The seepage and fracture-fed components are mixed in a karst store before discharging to the cave with the modelled dripwater $\delta^{18}O$ composition. By request the authors can supply the forward model as an excel spread sheet.

We performed sensitivity analyses on the model, changing the mean and standard deviation of the seepage reservoir flow time and the threshold values for recharge to the seepage reservoir and fracture flow, as follows. In order to reflect the observed lag in drip hydrology response to piston flow (Tooth and Fairchild, 2003) and seasonal recharge patterns we optimized our model

Hydrol. Earth Syst. Sci. Discuss., doi:10.5194/hess-2016-1, 2016
Manuscript under review for journal Hydrol. Earth Syst. Sci.
Published: 19 January 2016

to fit our observations of a mean 9-month delay and a standard deviation of 3 months. We then varied seepage and fracture thresholds and ran multiple scenarios in order to replicate a response in dripwater isotopic composition which could be accounted for by climate and bedrock limits alone. Results of various scenarios are explained in section 5.2.

Hydrol. Earth Syst. Sci. Discuss., doi:10.5194/hess-2016-1, 2016
Manuscript under review for journal Hydrol. Earth Syst. Sci.
Published: 19 January 2016

Hydrology and Earth System Sciences
Open Access
Discussions

209 ## 5 Results

210 A time series of monthly P – AET, cumulative water balance (CWB), discharge, dripwater
211 $\delta^{18}O$, and ion concentrations for Sites 1a and 2a from August 2005 – March 2011 are shown in
212 Figure 3.

213

214 ### 5.1. Water balance

215 Firstly, we observe a distinct seasonality in the potential water availability (P – AET) (Fig. 3A),
216 where winter months generate an excess (P > AET), while summer months generate a deficit
217 (P < AET) in in the soil water availability. Further, CWB shows three distinct trends throughout
218 the monitoring period: 1) a decline over the period of January 2006 to June 2006, consistent
219 with very low excess in P - AET; 2) an overall rise from June 2006 to February 2010; 3) a
220 decrease in P - AET from February 2010 to September 2010. Site 1a and 2a display moderate
221 and similar discharge rates, at the start of the monitoring period that continue until July 2006;
222 Site 1a an average of 90 ml ± 21 per week and Site 2a an average of 92 ml ± 23 per week. This
223 coincides with infiltration indicated by positive CWB (Fig. 3B). In July 2006, Site 1a
224 dramatically increases discharge five-fold to 468 ml/week on one cave visit, but had decreased
225 to 55 ml ± 3 ml per week on the subsequent visit two weeks later and was completely dry, three
226 months later. This site has not re-activated since (Department Parks and Wildlife, pers. comm.).
227 Site 2a shows much less variation in discharge overall, but contains smooth long-term trends.
228 Two periods of higher discharge are observed in August 2005 to May 2006 (average 92 ml ±
229 23 ml per week) and April 2008 to February 2009 (average 93 ml ± 29 ml per week), coinciding
230 with positive trends in CWB.

231

232

Hydrol. Earth Syst. Sci. Discuss., doi:10.5194/hess-2016-1, 2016
Manuscript under review for journal Hydrol. Earth Syst. Sci.
Published: 19 January 2016

Hydrology and Earth System Sciences
Discussions

233 **5.2 Water isotopes**

234 Dripwater $\delta^{18}O$ from Site 1a (Fig. 3C) shows no seasonal pattern but we see a steady increase
235 of 1‰ to January 2007, then a further steeper rise of 1.5‰ in June 2007, after which the drip
236 ceases. Dripwater $\delta^{18}O$ from Site 2a presents an overall increasing trend rising from -3‰ to +
237 0.7‰ over the monitoring period with a six-month quasi-seasonal signal (approx. 2‰ range)
238 that peaks from May/June to November/December generally coinciding with months when
239 infiltration from rainfall occurs. We hypothesise that the P < AET environment in drier summer
240 months isotopically enriches soil water, but this only arrives at the cave when seepage
241 thresholds are exceeded in periods of P > AET (winter months).

242

243 We undertook forward modelling of the dripwater $\delta^{18}O$ data from our rainfall isotopic data.
244 Our sensitivity analyses showed that seepage threshold values greater than 30 mm resulted in
245 the seasonal cessation of dripwater, which is not observed at our sites, thus the seepage
246 threshold is < 30 mm. Next we varied the fracture threshold between 10 and 1000 mm, the
247 wide range reflecting our uncertainty over this parameter. Given seepage flow is more
248 dominant in these highly porous highly calcarenite host rocks (Treble et al., 2003) we set our
249 chosen forward model to have a low threshold of 15 mm for seepage flow and a higher fracture
250 threshold of 100 mm to allow for dominant seepage flow but also some fracture flow in time
251 of high recharge. We set a 9 ± 3 month transit time for water from the surface to dripwater to
252 account for seasonal P – AET recharge forcing (Fig. 4). The mean of our forward-modelled
253 dripwater $\delta^{18}O$ (15 – 100 mm) is -3.98‰, less than the mean of Perth rainfall (-3.1‰) and
254 higher than the mean regional groundwater composition (-4.68‰). The time series of modelled
255 dripwater $\delta^{18}O$ (Fig. 3C) falls from -4.7 to -5.2 ‰ from the beginning of monitoring until
256 January 2007, but rises to -3.3‰ in January 2009, then rises to around -2‰ until Jan 2010

Hydrol. Earth Syst. Sci. Discuss., doi:10.5194/hess-2016-1, 2016
Manuscript under review for journal Hydrol. Earth Syst. Sci.
Published: 19 January 2016

when it finally declines to -3.2‰ at the end of the monitoring period. This chosen 15 mm – 100 mm threshold scenario (Fig. 4) and all other modelled scenarios show a gentle increasing trend, suggesting enrichment – a possible drying trend. Even when incorporating this slight increasing $\delta^{18}O$ trend, the difference between both our observed sites and modelled $\delta^{18}O$ dripwater threshold scenarios at statistically significant (Table 1; detailed below).

The slopes in the measured $\delta^{18}O$ time-series at Site 1a (0.13‰ /month) and Site 2a (0.05‰ /month) are both higher than that of the climatically-driven forward modelled dripwater $\delta^{18}O$ (0.03‰ /month) and there are considerable differences between the sites in their response. In all meaningful modelled scenarios (Fig. 3), taking into account climate and bedrock hydrologic processes, observed dripwater compositions are significantly more enriched than forward modelled $\delta^{18}O$. This is demonstrated through our t-test which set out to determine if the difference between observed $\delta^{18}O$ at each site and forward modelled $\delta^{18}O$ is statistically significant. The results of our test (Table 1) show both sites are significantly different from modelled $\delta^{18}O$. It is also well-above the mean $\delta^{18}O$ for cave dripwater at Golgotha Cave (-3.9‰; Treble et al, 2013). Figure 5 shows that cave dripwater isotopic enrichment occurs along a least squares regression (LSR) that falls within the standard error (± 0.45‰) of the slope for the local meteoric water line (LMWL, weighted LSR). This confirms a *type 1* scenario suggested by Cuthbert et al., (2014) where a single water source dominates cave dripwater and shows increased near-surface evaporation in a humid subsurface environment (> 95% relative humidity).

5.3 Water Solutes

There are significant differences in solute concentrations and trends between the two sites (Fig. 3E, 3F, 3G and 3H). Solute concentrations are typically higher at Site 1a versus Site 2a and

Hydrol. Earth Syst. Sci. Discuss., doi:10.5194/hess-2016-1, 2016
Manuscript under review for journal Hydrol. Earth Syst. Sci.
Published: 19 January 2016

they demonstrate opposite trends post-fire. At Site 1a, Cl, Ca, Mg and Sr decline overall, although this trend is step-wise for Ca, and reverses for Cl ~ 6 months before the drip ceases. The trends in these solutes are inconsistent with that expected from climate and the observed CWB (Fig 3A). Solute concentrations decrease with decreasing CWB, where as a decrease in CWB should result in an increase in solute concentrations, as a result of up-concentration of solutes in response to evaporation. We also note that initial Cl and other solute concentrations at Site 1a are twice that at Site 2a, and there are tree roots visible above Site 1a and not at Site 2a, indicating these may be effecting dripwater composition by concentrating solutes. Furthermore at Site 2a Cl and other solute concentrations show a direct relationship to CWB (i.e. increasing solute concentration with decreasing CWB and decrease with increasing CWB).

Trends in SO_4 and K are more subtle than for other solutes, K only shows a slight decline prior to Site 1a ceasing to drip and SO_4 appears to be slightly increasing, although our SO_4 time series is shorter. Similarly, trends in SO_4 and K for Site 2a are subtle, although they are slightly increasing through time. K and SO_4 concentrations are again, 2 - 3 times higher at Site 1a versus Site 2a and are considerably higher than those recorded at Golgotha Cave (Table 2) whilst concentrations for other solutes between these cave sites are more comparable.

In summary, while post-fire solute concentrations at Yonderup, are typically higher at Site 1a versus Site 2a, they demonstrate opposite trends post-fire. While Site 2a solutes demonstrate a direct relationship with climate driven CWB, at Site 1a, they show a more complex relationship, which we argue is largely influenced by changes in a combination of local factors including vegetation change, discharge and evaporation post-fire.

Hydrol. Earth Syst. Sci. Discuss., doi:10.5194/hess-2016-1, 2016
Manuscript under review for journal Hydrol. Earth Syst. Sci.
Published: 19 January 2016

Hydrology and Earth System Sciences
Open Access
Discussions

303

304 # 6 Discussion

305

306 ## 6.1 Post-fire hydrology

307 Discharge at Site 1a is inconsistent with CWB: discharge rose as rainfall fell below the long-
308 term mean (P < AET) (Fig. 3A and 3B), suggesting that Site 1a received a localised increase
309 post-fire in available water despite the declining input from rainfall. In contrast, discharge at
310 Site 2a post-fire is related more directly to the cumulative water balance (CWB), with higher
311 discharge coinciding with periods of higher water surplus suggesting a simple hydrological
312 response driven by infiltration. These post-fire observations are consistent with dripwater Cl
313 and other solutes at Yonderup. Chloride is a chemically conservative solute (Graedel and
314 Keene, 1996), hence its concentration in dripwater will primarily be a function of physical
315 processes such as dilution, mixing (Tooth and Fairchild, 2003; Tremaine and Froelich, 2013)
316 and potentially evaporation and transpiration (Treble et al., in prep).

317 We propose that Cl concentrations at Site 2a increases during the period of declining CWB
318 due to increased evapotranspiration and that this trend is reversed when rainfall infiltration
319 increases (P > AET) causing dilution (Fig. 3E). Similarly, the rise in discharge at Site 1a
320 coincided with falling Cl concentrations suggesting dilution. However, since this cannot be due
321 to increased rainfall, a different mechanism is required to explain the dilution of Cl at Site 1a.
322 During the fire, a large Tuart tree, growing above Site 1a (within 5 m according to our survey),
323 was destroyed. Transpiration by deeply-rooted trees in this environment has been implicated
324 in producing high Cl concentrations in the unsaturated zone (Turner et al., 1987) and the impact
325 of this process on dripwater at Golgotha Cave has been demonstrated, with dripwater Cl
326 concentrations being at least five times higher than rainfall concentrations owing to ion
327 exclusion during transpiration. This coupled with the initial concentration of Cl at Site 1a (Tuart

Hydrol. Earth Syst. Sci. Discuss., doi:10.5194/hess-2016-1, 2016
Manuscript under review for journal Hydrol. Earth Syst. Sci.
Published: 19 January 2016

tree) being double that of Site 2a (no Tuart tree) we believe transpiration is largely controlling Cl concentrations at this site. Thus we propose that a reduction in localised transpiration, and consequently an increase in discharge following the fire, is driving the dilution that lead to a decline in Cl at Site 1a. Moreover, post-fire Cl values at the shallow Yonderup Cave, are more than double baseline Cl concentrations from groundwater and cave sites such as Golgotha Cave (Table 2). The Cl response at both sites strongly suggests fire can alter dripwater Cl by altering transpiration and evaporation rates. The impact of this on the dripwater chemistry is discussed further and a conceptual model devised later in this section.

6.2 Post-fire carbonate chemistry

Similar to Cl, declining concentrations of carbonate metals (Mg, Ca and Sr) at Site 1a reflect dilution that we interpret as a reduction in post-fire transpiration owing to the death of the tuart tree. We interpret that the rising trend at Site 2a reflects increasing solute concentrations due to a rise in post-fire evapotranspiration owing to vegetation recovery and evaporation of near-surface water stores (Fig. 3F, 3G and 3H respectively). Additionally, Ca concentrations at Site 1a decrease in a non-linear fashion (Fig. 3G), with a step-like decrease each autumn suggesting that a further mechanism, in addition to dilution, is contributing to falling dripwater Ca concentrations at Site 1a.

There are a number of mechanisms that could influence post-fire Ca concentrations, including: (1) increased evaporation in the near-surface inducing prior calcite precipitation (PCP) shown by the diagnostic model for water-rock interactions that includes PCP in Figure 6 (Fairchild et al., 2000; Sinclair 2011; Treble et al., 2015). (2) A decrease in the amount of microbial and root respiration, which have both been implicated as a significant source of CO_2 (Coleborn et al., 2016; Treble et al., 2015) and hence a decrease in carbonic acid and a decrease in dissolved

Hydrol. Earth Syst. Sci. Discuss., doi:10.5194/hess-2016-1, 2016
Manuscript under review for journal Hydrol. Earth Syst. Sci.
Published: 19 January 2016

352 Ca from lower carbonate mineral dissolution by carbonic acid. (3) The addition of plant ash
353 (Yusiharni and Gilkes, 2012a) and highly soluble CaO, produced by the burning of exposed
354 surface rock to the fire (Yusiharni and Gilkes, 2012b) to the soil profile, could influence Ca
355 availability through leaching over time in dripwater. The relative importance of these three
356 processes is difficult to assess in our data; processes (1) and (2) cannot be constrained as our
357 in-cave pCO_2 data is limited while for (3) the addition of plant ash and CaO would increase Ca
358 availability in cave dripwater, however it is unclear whether this would be reflected in
359 dripwater composition as (1) and (2), which are not constrained can alter Ca concentrations, as
360 they influence cave dripwater after (3). For example: the death of the tuart tree may have
361 reduced in-cave pCO_2 from roots – a key driver of Ca concentrations - thus reducing Ca
362 concentrations in the dripwater. However as previously stated it is difficult to constrain a
363 particular mechanism that is controlling the composition of Ca at Site 1a.

364 Sulphate and K post-fire at Site 1a show abnormally high SO_4 and K (Fig. 3H and 3I), and an
365 increase in SO_4 concentrations which is counterintuitive to the initial dilution signal (owing to
366 reduced transpiration) interpreted for the other solutes. While at Site 2a, SO_4 and K show an
367 increase similar to other solutes and can be explained by the inferred increase in
368 evapotranspiration. The SO_4 and K response at Site 1a suggests an additional process is
369 affecting SO_4 and K concentrations post-fire (Fig. 3H and 3I). The majority of aboveground
370 SO_4 is predominantly stored within the lower to middle storey of the forest (O'Connell and
371 Grove, 1996) and post-fire soils have been found to contain 23% more S and 16% more K than
372 pre-fire soils due to biomass-sourced ash deposition (Grove et al., 1986). Thus differences in
373 biomass above the two sites may explain the high concentrations at Site 1a and differences in
374 between drip site SO_4 and K concentrations post-fire. We suggest dripwater SO_4 and K at Site
375 1a maintains relatively high constant concentrations (Fig. 3H and 3I) due to increased source
376 input (from burnt vegetation and litter) until the increase in near surface evaporation from 2007

Hydrol. Earth Syst. Sci. Discuss., doi:10.5194/hess-2016-1, 2016
Manuscript under review for journal Hydrol. Earth Syst. Sci.
Published: 19 January 2016

377 onwards that drives even higher concentrations mimicking the Cl and $\delta^{18}O$ trend. This is
378 consistent with Site 2a, which has much less biomass above the site and thus lower initial SO_4
379 and K concentrations, further these solutes show a steady increasing trend that is consistent
380 with increased evapotranspiration post-fire displayed in other solutes. We compare our
381 Yonderup results to Golgotha to put SO_4 and K concentrations into context. Lower
382 concentrations of SO_4 at Golgotha Cave, which last experienced a wildfire in 1992 and a
383 prescribed burn in 2006, strongly suggest that Yonderup has comparatively high concentrations
384 of SO_4 and K (Table 2). Given the high intensity of the wildfire and the large amount of
385 resulting ash deposited, we suggest that these high concentrations reflect the intensity of the
386 fire and the biomass burnt above Yonderup (Grove et al., 1986).

387

388 **6.3 A multi-proxy fire signal in dripwater**

389 Here we propose post-fire scenarios for both sites at Yonderup (refer to conceptual model Fig.
390 7) that account for the observed dripwater chemistry that have been shown to be altered by
391 local, changes in the surface soil/vegetation/hydrology initiated by an intense wildfire. A
392 relatively straight-forward relationship between CWB, discharge and Cl concentrations at Site
393 2a, suggests increased concentration of solutes (Ca, Mg, Sr, K and SO_4) in response to an
394 increase in near-surface evaporation (Fig. 3C and 3D). At Site 1a, we hypothesize both the
395 death of the tuart tree in the wildfire - which resulted in a reduction of transpiration - and a
396 subsequent increase in rainfall infiltration lead to an initial dilution of solutes causing a
397 decrease in Cl, Mg, Ca and Sr concentrations. This is supported by the modelled $\delta^{18}O$ agreeing
398 with dripwater $\delta^{18}O$ until 2007 (Fig. 3).

399 Tuart tree transpiration at the surface and subsurface ranges from -0.86 ± 0.11 MPa in the
400 summer to -0.35 ± 0.02 MPa in the winter (Drake et al., 2011). We suspect this potential created

Hydrol. Earth Syst. Sci. Discuss., doi:10.5194/hess-2016-1, 2016
Manuscript under review for journal Hydrol. Earth Syst. Sci.
Published: 19 January 2016

Hydrology and Earth System Sciences
Discussions

by transpiration was creating a positive hydraulic gradient towards Site 1a and maintaining high concentrations of Cl (the conservative solute) in dripwater. Post-fire a multitude of processes such as the increase in discharge, the decrease in transpiration, the increase in near-surface evaporation and post-fire ash deposition explain the various trends observed in dripwater chemistry. Trends such as the gradual decline in concentrations of Cl, Mg and Sr that reflect dilution and the decrease in transpiration and the consistently high SO_4 and K concentrations that are largely attributed to post-fire ash deposition (Grove et al., 1986). Accordingly, the combination of a lower hydraulic gradient and a higher evaporation rate – reflected by the sharp increase in $\delta^{18}O$ post Jan 2007 - resulted in depletion of the near-surface reservoir feeding Site 1a, and subsequently an inactivation of the drip site.

At Site 2a there was a lower-middle understory above the site that was burnt during the fire. We propose that the loss of this lower-middle understory increased the near-surface evaporation signal and initially decreased transpiration but as lower storey vegetation recovered an increase in transpiration and a high evaporation rate (still due to a low albedo and limited forest litter) resulted in the increasing concentration of solutes (Cl, Mg, Ca, and Sr) and $\delta^{18}O$ (Fig. 3E, 3F, 3G and 3H) at Site 2a. In contrast at Site 1a various factors including: dilution, the reduction of canopy cover from the tuart tree coupled with a reduction in albedo (blackened soil, Fig. 1) from the fire, may have contributed to higher surface temperatures resulting in evaporation-driven high $\delta^{18}O$ values. However, the reduction in transpiration due to the death of tree eventually caused a decline in solutes.

Hence we propose that differences in surface vegetation above sites influence site specific drip chemistry, for example; Site 1a has a larger driver of transpiration - the tuart tree - which died during the fire and subsequently influences discharge post-fire, while at Site 2a the fire impact is limited to understorey shrub vegetation and discharge is much less influenced post-fire.

Hydrol. Earth Syst. Sci. Discuss., doi:10.5194/hess-2016-1, 2016
Manuscript under review for journal Hydrol. Earth Syst. Sci.
Published: 19 January 2016

425 Furthermore, a larger abundance of biomass - the tuart tree - at Site 1a and an increase in
426 leaching as a result of increased discharge can account for high concentrations of SO_4 and K at
427 Site 1a, while less biomass above Site 2a, a stable low discharge and predominantly near-
428 surface evaporation and transpiration dominated response accounts for lower concentrations of
429 SO_4 and K at Site 2a. While this heterogeneity in response between the two sites at Yonderup
430 is significant, so too is the comparison between Yonderup drip chemistry and the drip chemistry
431 at Golgotha, which – more generally - highlights that, despite site specific variation, an intense
432 wildfire has multi-year effects on dripwater composition in shallow caves post-fire.

433

434 **7 Conclusions and avenues for future research**

435 We isolate a post-wildfire response by comparing a recently burnt cave monitoring site with
436 baseline values of local pre-fire, groundwater and nearby cave monitoring data. We provide a
437 novel analysis of the multi-year impacts wildfire has on cave dripwater. Our analysis shows a
438 strong hydrologic relationship between surface environments and shallow caves that are
439 located within the tree rooting zone. This finding is especially important in water-limited
440 environments (P < ET) as the overlying vegetation can exert controls on the cave
441 hydrogeochemical environment. The post-wildfire dripwater response is clearest in $\delta^{18}O$ and
442 Cl due to their sensitivity to changes in near-surface evaporation and SO_4 and K due to their
443 leaching from the ash. Other solutes such as Mg, Sr and Ca support these conclusions when
444 using a multi-proxy approach.

445 We propose a conceptual model for a multi-year post-wildfire cave dripwater response in
446 forested water-limited regions. This involves a 5 - 10 yr response of: 1) higher $\delta^{18}O$ and Cl in
447 cave dripwater due to increased evaporation and decreased shading soon after the wildfire; 2)
448 increased K and SO_4 due to the leaching of biomass-sourced ash; and 3) increased variability

Hydrol. Earth Syst. Sci. Discuss., doi:10.5194/hess-2016-1, 2016
Manuscript under review for journal Hydrol. Earth Syst. Sci.
Published: 19 January 2016

449 in Mg, Sr and Ca due to changes in evaporation, transpiration and water-rock interactions post-
450 fire. We would expect a full recovery within 10 - 20 years after the wildfire and a return to pre-
451 fire isotopic, major and trace element concentrations as a result of revegetation growth (Treble
452 et al., submitted) and re-establishment of the pre-fire albedo.

453 Our post-wildfire dripwater response from $\delta^{18}O$ shows ~ 2‰ increase - relative to forward
454 modelled climate $\delta^{18}O$, regional groundwater and Golgotha Cave $\delta^{18}O$ data. If preserved at
455 equilibrium this is equivalent to some of the largest changes seen in the Quaternary record.
456 This highlights the significance of a fire signal that could be misinterpreted as climate
457 variability especially when combined with other proxies that would also be affected by fire,
458 such as speleothem growth rate. Furthermore, the potential preservation of a unique fire
459 signature of $\delta^{18}O$, S and Cl in speleothems, combined with trace elements (Mg, Sr), opens a
460 new avenue for research into paleo-fire records.

461

Hydrol. Earth Syst. Sci. Discuss., doi:10.5194/hess-2016-1, 2016
Manuscript under review for journal Hydrol. Earth Syst. Sci.
Published: 19 January 2016

Hydrology and Earth System Sciences
Open Access
Discussions

Acknowledgements

Many thanks must go to the team at Yanchep National Park, especially Ciara McDuff, Rob Foulds and Gary Hunton for your assistance with the data collection. We also acknowledge ANSTO staff: Alan Griffith (AWAP data access, Suzanne Hollins for permission to use unpublished Perth rainfall isotopic data, Henri Wong, Scott Allchin and Barbora Gallager for dripwater analyses; as well as Michael Gagan and Joan Cowley for assistance with water isotopes at ANU. This research was in part funded by ARC Linkage LP13010017 and Land & Water Australia grant (ANU52) to PT. The outcomes of this study contribute to ARC Discovery Project DP140102059 awarded to PT. This research was also supported by the AINSE honours scholarship program awarded to GN.

Hydrol. Earth Syst. Sci. Discuss., doi:10.5194/hess-2016-1, 2016
Manuscript under review for journal Hydrol. Earth Syst. Sci.
Published: 19 January 2016

References

Abbott, I., and Burrows, N.: Fire in ecosystems of south-west Western Australia: impacts and management, Backhuys., 2003.

Baker, A., Asrat, A., Fairchild, I. J., Leng, M. J., Thomas, L., Widmann, M., Jex, C. N., Dong, B., van Calsteren, P., Bryant, C.: Decadal-scale rainfall variability in Ethiopia recorded in an annually laminated, Holocene-age, stalagmite, The Holocene, 20, 827 – 836, 2010.

Baker, A., Bradley, C.: Modern stalagmite $\delta^{18}O$: Instrumental calibration and forward modelling, Global Planet. Change, 71, 201-206, 2010. doi: 10.1016/j.gloplacha.2009.05.002

Coleborn K., Spate A., Tozer M., Andersen M S., Fairchild I J., MacKenzie B., Treble P C., Meehan S., Baker A., Baker A.: Effects of wildfire on long-term soil CO_2 concentration: Implications for karst processes, Envt. Earth Sci, 2016 (in press).

Collister, C., Mattey, D.: Controls on drop volume at speleothem drip sites: An experimental study, J. Hydro., 358, 259 – 267, 2008.

Cuthbert, M.O., Baker, A., Jex, C.N., Graham, P.W.,Treble, P.C., Andersen, M.S., and Ian Acworth, R., Drip water isotopes in semi-arid karst: Implications for speleothem plaeoclimatlogy, Earth and Planet. Sci. Lett., 395, 194-204, 2014. doi: 10.1016/j.epsl.2014.03.034.

Drake, P. L., Froend, R. H., and Franks, P.J.: Linking hydraulic conductivity and photosynthesis to water-source partitioning in trees versus seedlings, Tree Physiol., 31, 763-773, 2011.

Fairchild, I. J. and Baker, A.: Speleothem Science: From process to Past Environments., 2012.

498 Fairchild, I.J., Borsato, A., Tooth, A.F., Frisia, S., Hawkesworth, C.J., Huang, Y.,
499 McDermott, and Spiro, B.: Controls on trace element (Sr-Mg) compositions of carbonate
500 cave waters: implications for spelothem climatic records, Chem. Geol., 166, 255-269,
501 2000. doi: 10.1016/S0009-2541(99)00216-8.
502 Fairchild, I.J., and Treble, P.C.,: Trace elements in speleothems as recorders of environmetal
503 change, Quat. Sci. Rev., 28, 449-468, 2009. doi: 10.1016/j.quascirev.2008.11.007.
504 Gonzalez-Pelayo, O., Andreu, V., Gimeno-Garcia, E., Campo, J., and Rubio, J.L.: Effects of
505 fire and vegetation cover on hydrological characteristics of a Mediterranean shrubland
506 soil, Hydrol. Processes, 24, 1504-1513, 2010. doi: 10.1002/hyp.7612
507 Graedel, T.E., Keene, W.C.: The budget and cycle of Earth's natural chlorine, Pure and Appl.
508 Chem., 68, 1689-1697, 1996.
509 Grove, T. S., O'Connell, A. M., Dimmock, G. M.: Nutrient changes in surface soils after an
510 intense fire in jarrah (*Eucalyptus marginata*) forest, Aust. J. Ecol., 11, 303 – 317, 1986.
511 Hingston, F. J., Gailitis, V.: The geographic variation of salt precipitated over Western
512 Australia, Aust. J. Soil Res., 14, 319 – 335, 1976.
513 Hughes, C.E., and Crawford, J.: A new precipitation weighted method for determining the
514 metoric water line for hydrological applications demonstrated using Australian and
515 GNIP data, J. of hydro., 344-351, 2012. doi: 10.1016/j.jhydrol.2012.07.029.
516 Hurst, H.: Methods of long-term storage in reservoirs, Transactions of the American Society
517 of Civil Engineers, 116, 519 – 543, 1951.
518 Jennings, J. N.: Syngenetic Karstsin Australia *in* Williams, P. W. & J. N. Jennings (eds.),
519 Contributions to the study of Karst, Department of Geography Publication. G/5,
520 Australian National University, 41 – 110.
521 Lachinet, M.S.: Climatic and environmental controld on speleothem oxygen-isotope values:
522 Quat. Sci. Rev., 28, 412-432, 2009. doi: 10.1016/j.quascirev.2008.10.021.

523 O'Connell, A. M., Grove, T. S.: Biomass production, nutrient uptake and nutrient cycling in
524 the jarrah and karri forests of south-western Australia, Nutrition of Eucalypts, 155 – 189,
525 1996.
526 Mahmud, K., Mariethoz, G., Baker, A. Treble, P. C., Markowska, M., McGuire, L.:
527 Estimation of deep infiltration in unsaturated limestone environments using cave LiDAR
528 and drip count data, Hydrol. Earth Syst. Sci. Discuss., 19, 1-35, doi: 10.5194/hessd-12-
529 8891-2015.
530 Mcdermott, F., Mattey, D. P. & Hawkesworth, C.: Centennial-scale Holocene climate
531 variability revealed by a high-resolution speleothem δ18O Record from SW Ireland,
532 Science, 294, 1328–1332, 2001.
533 Pape, J.R., Banner, J.L., Mack, L.E., Musgrove, M., and Guilfoyle, A.: Controls on oxygen
534 isotope variability in precipitation and cave drip waters, central Texas, USA, J. of
535 Hydrology, 385, 203–215, 2010. doi: 10.1016/j.jhydrol.2010.02.021.
536 Raupach, M.R., Briggs, P.R., Haverd, V., King, E. a., Paget, M., and Trudinger, C.M.:
537 Australian Water Availability Project (AWAP), CSIRO Marine and Atmospheric
538 Research Component: Final Report for Phase 3, 1-72, 2009.
539 Raupach, M. R., Harman, I. N., Canadell, J. G.: Global climate goals for temperature,
540 concentrations, emissions and cumulative emissions, CSIRO CAWCR Technical Report
541 no. 42, 2011.
542 Rutlidge, H., Baker, A., Marjo, C.e., Andersen, M.S., Graham, P.W., Cuthbert, M.O.,
543 Rau,G.C., Roshan, H., Markowska, M., Marithoz, G., and Jex, C.N.: Dripwater organic
544 matter and trace element geochemistry in a semi-arid karst environment: Implications for
545 speleothem paleoclimatology, Geochimica et Cosmochimica Acta, 135, 217–230, 2014.
546 doi: 10.1016/j.gca.2014.03.036.

547 Silberstein, R.P., Dawes, W.R., Bastow, T.P., Byrne, J., Smart, N.F.: Evaluation of post-fire
548 recharge under native woodland using hydrological measurements, modelling and
549 remote sensing: Journal of Hydrology, 489, 1-15, 2013.
550 Sinclair, D.J., 2011, Two mathematical models of Mg and Sr partitioning into solution during
551 incongruent calcite dissolution, Chemical Geology, v. 283, p. 119-133.
552 Tooth, A. F. and Fairchild, I. J.: Soil and karst aquifer hydrological controls on the
553 geochemical evolution of speleothem-forming drip waters, Crag Cave, southwest
554 Ireland, J. Hydrol., 273, 51–68, doi:10.1016/S0022-1694(02)00349-9, 2003.
555 Treble, P.C., Bradley, C., Wood, A., Baker, A., Jex, C.N., Fairchild, I.J., Gagan, M.K.,
556 Cowley, J., and Azcurra, C.: An isotopic and modelling study of flow paths and storage
557 in Quaternary calcarenite, SW australia: implications for speleothem paleoclimate
558 records: Quat. Sci. Rev., 64, 90-103, 2013. doi: 10.1016/j.quascirev.2012.12.015.
559 Treble, P.C, Fairchild, I. J., Griffiths, A., Baker, A., Meredith, K. T., Wood, A., McGuire, E.:
560 Impacts of cave air ventilation and in-cave prior calcite precipitation on Golgotha cave
561 drip water chemistry, southwest Australia, Quat. Sci. Rev., 2015 (in press).
562 Treble, P. C., Fairchild, I. J., Baker, A., Meredith, K. M., Andersen, M. S., Salmon, S. U.,
563 Bradley, C., Wynn, P. M., Hankin, S., Wood, A., McGuire, E.: Roles of bioproductivity,
564 transpiration and fire in an eight-year record of cave dripwater chemistry from a forested
565 catchment, southwest Australia, 2015. (submitted)
566 Tremaine, M. D., Froelich, N. P.: Speleothem trace element signatures: A hyrologic
567 geochemical study of modern cave dripwaters and farmed calcite, Geochimica et
568 Cosmochimica Acta, 121, 522 – 545, 2013. doi:10. 1016/j.gca.2013.07.026
569 Turner, J. V., Arad, A., Johston, C. D.: Environmental isotope hydrology of salanized
570 experimetal catchments, Journal of Hydrology, 94, 89-107, 1987. doi: 10.1016/0022-
571 1694(87)90034-5.

572 Turner, J.V., Thorpe, P.M.: Paleotemperature conditions for the southwest of Western
573 Australia from the stable isotopic composition of deep, confined groundwater within the
574 Perth Basin: Proceedings of International Conference on the Study of Environmental
575 Change using isotope techniques, 23-26 April 2001, Vienna: IAEA: 504-508, 2001.
576 Watts, A. R., and Henley, P. W.: Map of Yonderup Cave, Cave Research Group, scale 1: 100,
577 1973.
578 Wong, C., and Banner, J. L.: Response of cave air CO2 and drip water to brush clearing in
579 central Texas: Implications for recharge and soil CO2 dynamics, J. Geophys. Res., 115,
580 G04018, 2010. doi:10.1029/2010JG001301.
581 Woodhead, J. et al.: Speleothem climate records from deep time? Exploring the potential with
582 an example from the Permian, Geology, 38, 455–458, 2010.
583 Yusiharni, E., and Gilkes, R.J.: Changes in the mineralogy and chemistry of a lateritis soil
584 due to a bushfire at Wundowie, Darling Range, Western Asutralia, Geoderma, 191, 140-
585 150, 2012(a). doi: 10.1016/j.geoderma.2012.01.030.
586 Yusiharni, E., and Gilkes, R.J.: Minerals in the ash of Australian native plants, Geoderma,
587 189-190, 369-380, 2012(b).
588
589
590
591
592
593
594
595
596

Hydrol. Earth Syst. Sci. Discuss., doi:10.5194/hess-2016-1, 2016
Manuscript under review for journal Hydrol. Earth Syst. Sci.
Published: 19 January 2016

Hydrology and Earth System Sciences
Open Access
Discussions

597 Table 1. Summary of two sample t-test of Site 1a and 2a $\delta^{18}O$ values in Figure 2D against
598 forward modeled $\delta^{18}O$.

Variable	Number of samples	Mean	Standard deviation	P - value	Significance (P< 0.05)
Site 1a	23	-2.80	0.94	0.002	Yes (P > 0.05)
Site 2a	41	-1.56	0.83	<0.001	Yes (P < 0.05)
Modelled	72	-3.58	1.23		

599

600

601

Hydrol. Earth Syst. Sci. Discuss., doi:10.5194/hess-2016-1, 2016
Manuscript under review for journal Hydrol. Earth Syst. Sci.
Published: 19 January 2016

Hydrology and Earth System Sciences
Discussions
Open Access
EGU

602 Table 2. A summary table comparing the hydrogeochemistry of, (A) shallow Yonderup drip sites burnt in a 2005 wildfire to; (B) deeper
603 Golgotha cave sites burnt in a 1992 wildfire and a 2006 prescribed burn; (C) unpublished Perth rainfall data during the monitoring period
604 (ANSTO); (D) rainfall isotopic composition (Turner and Thorpe, 2001); (E) groundwater isotopic composition (Turner and Thorpe, 2001); (F)
605 Yanchep rainfall solute composition (Hingston and Gailitis, 1976).

606

Location		Discharge (ml/day)	Ca (mmol/L)	Mg (mmol/L)	Sr (mmol/L)	Cl (mmol/L)	SO_4^{2+} (mmol/L)	K (mmol/L)	$\delta^{18}O$ (per mil)	n
(A) Yonderup										
Site 1A	Median	12.2	1.2	0.46	0.01	8.1	0.25	0.15	-3.2	27
	SD	2.6	0.6	0.13	0.2×10^{-2}	0.6	0.02	0.03	1.23	
Site 2A	Median	6.1	1.42	0.37	0.01	5.91	0.14	0.05	-1.48	49
	SD	4.8	0.2	0.04	0.5×10^{-3}	1.75	0.05	0.8×10^{-2}	0.84	
(B) Golgotha										
Site 1A	Median	63	1.2	0.3	0.2×10^{-2}	3.35	8.0×10^{-2}	0.02	-4.1	85
	SD	4.7	0.22	0.03	0.183×10^{-3}	0.18	0.4×10^{-2}	0.3×10^{-2}	0.3	
Site 1B	Median	40	1.1	0.3	0.2×10^{-2}	3.41	8.0×10^{-2}	2.3×10^{-2}	-3.9	82
	SD	2.0	0.25	0.03	2.39×10^{-4}	0.25	0.5×10^{-2}	0.5×10^{-2}	0.1	
Site 2A	Median	47	1.1	0.32	0.2×10^{-2}	2.76	0.13	3.8×10^{-2}	-3.9	77
	SD	10	0.25	0.02	0.1×10^{-3}	0.22	0.8×10^{-2}	0.5×10^{-2}	0.1	
Site 2B	Median	67	1.22	0.33	0.2×10^{-2}	4.49	9.8×10^{-2}	3.8×10^{-2}		84
	SD	85	0.27	0.03	0.2×10^{-3}	0.24	0.6×10^{-2}	0.7×10^{-2}		
Site 2E	Median	524	1.9	0.31	0.1×10^{-3}	4.11	0.085	3.8×10^{-2}		51
	SD	45	0.2	0.02	0.2×10^{-3}	0.17	0.4×10^{-2}	0.4×10^{-2}		
(C) ANSTO Rainfall	*Mean*								-3.1	64
(D) CSIRO long term rainfall (Perth)	*Mean*								-3.85	165
(E) Regional groundwater (Perth)	*Mean*								-4.68 0.4	43
(F) Yanchep Rainfall Solutes	*Mean*		0.008			0.01	0.1×10^{-2}	0.4×10^{-2}		

Hydrol. Earth Syst. Sci. Discuss., doi:10.5194/hess-2016-1, 2016
Manuscript under review for journal Hydrol. Earth Syst. Sci.
Published: 19 January 2016

607

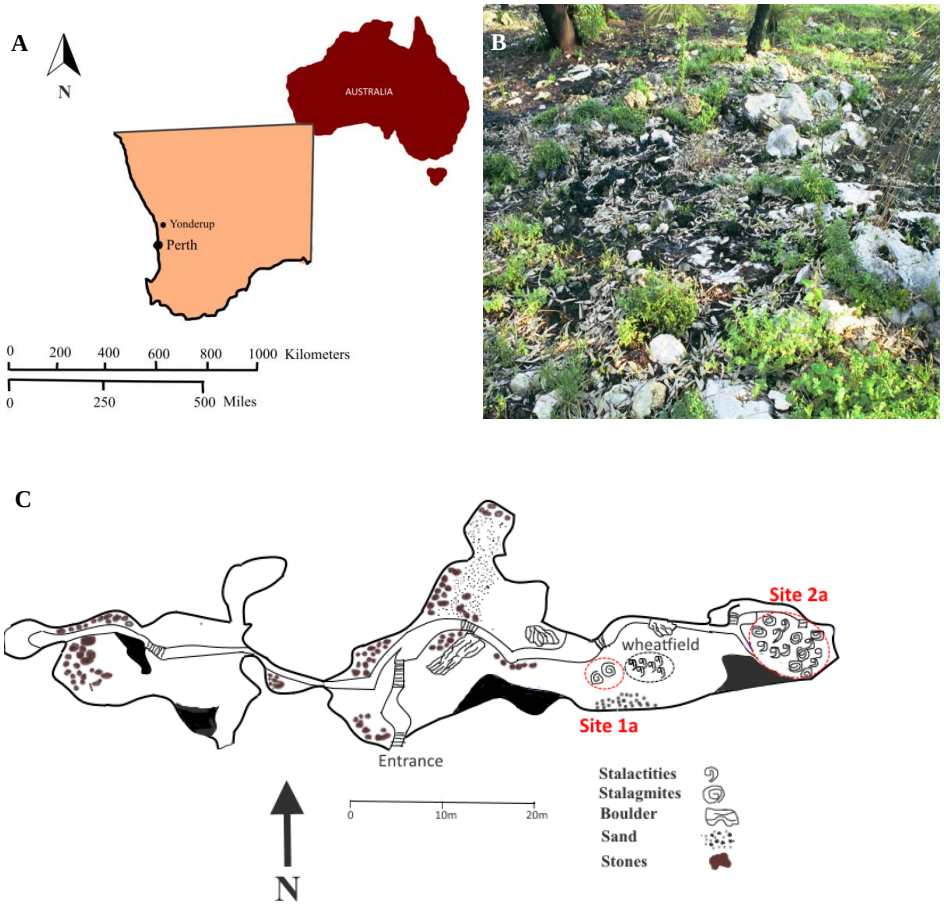

608

609 Figure 1. Shows the geographical location of our study site (A), a post fire photograph of the
610 area (B) taken in August 2005 a photo of recovering shrubs and grass post wildfire, and (C) a
611 map of Yonderup cave to scale originally surveyed by Watts and Henley, (1973).

612

613

614

Hydrol. Earth Syst. Sci. Discuss., doi:10.5194/hess-2016-1, 2016
Manuscript under review for journal Hydrol. Earth Syst. Sci.
Published: 19 January 2016

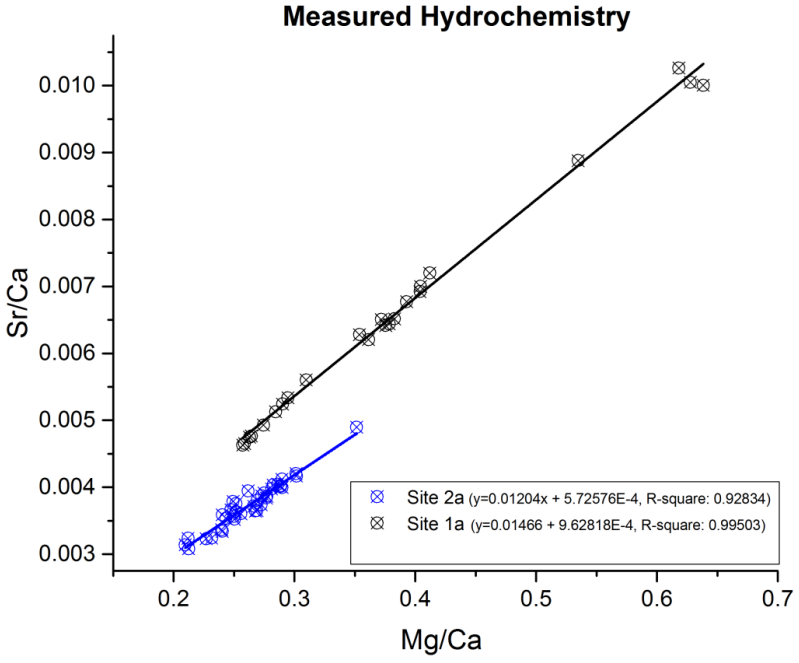

615

616 Figure 2. Relationship between Sr/Ca vs Mg/Ca for both Site 1a (black) and Site 2a (blue), this

617 indicates that both sites have independent flow paths.

618

619

620

621

Hydrol. Earth Syst. Sci. Discuss., doi:10.5194/hess-2016-1, 2016
Manuscript under review for journal Hydrol. Earth Syst. Sci.
Published: 19 January 2016

Hydrology and Earth System Sciences
Discussions

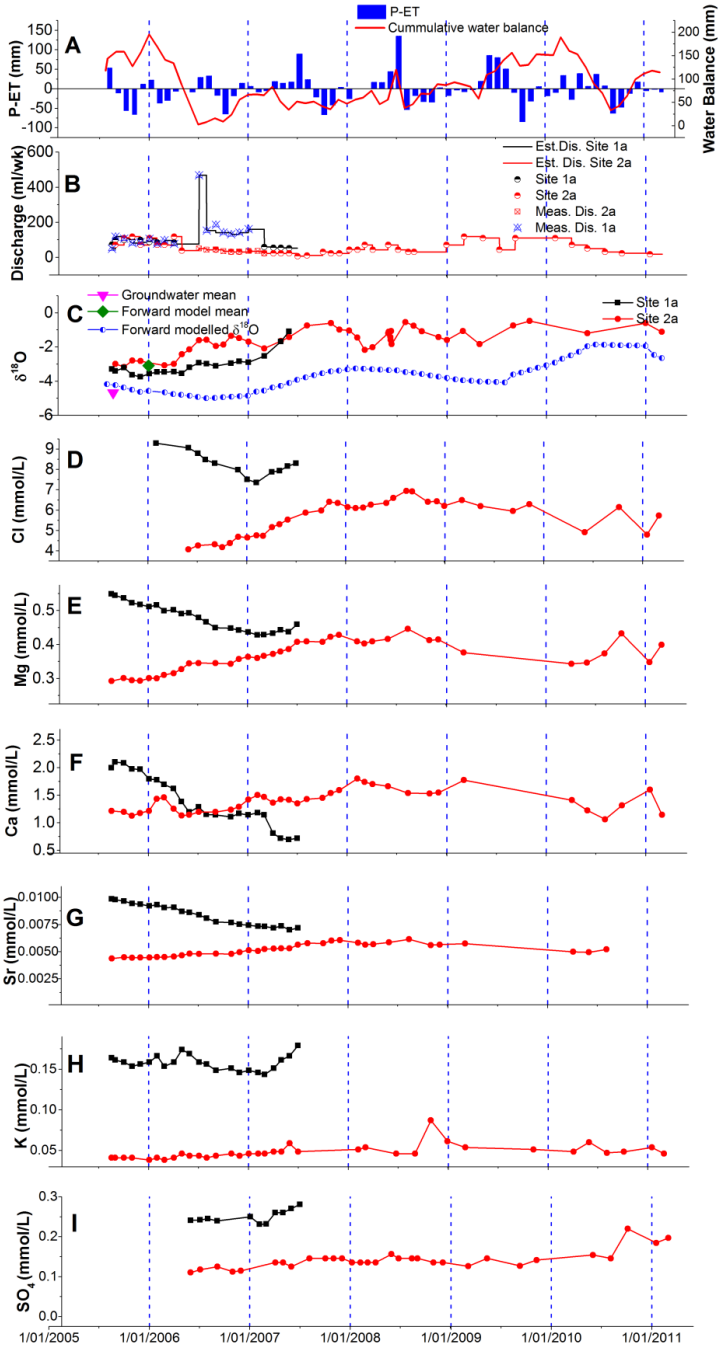

622

Hydrol. Earth Syst. Sci. Discuss., doi:10.5194/hess-2016-1, 2016
Manuscript under review for journal Hydrol. Earth Syst. Sci.
Published: 19 January 2016

Hydrology and Earth System Sciences
Discussions

623 Figure 3. Presents a post-fire time series analysis of Site 1a and Site 2a. Note: Site 1a dries up
624 in June 2007. (A) Precipitation – actual evapotranspiration (P – AET), shows seasonal
625 variations of excess (above threshold) and deficiency (below threshold) on a monthly scale
626 overlayed with cumulative surface water balance. (B) Discharge is given in ml/week actual
627 measured discharge data is given as Meas. Dis. 1a and 2a, while calculated data is given as
628 Site 1a and Site 2a this is then inferred to give our estimated measured discharge (Est. Dis.
629 Site 1a and Site 2a). Site 1a shows a spike in measured discharge in August 2006 and a
630 consequent decrease until the site is dry, while Site 2a shows little variability in discharge
631 throughout the monitoring period. (C) Shows observed $\delta^{18}O$ composition of cave dripwater
632 from Site 1a and Site 2a with the forward modelled $\delta^{18}O$ (15 – 100 mm; blue) and mean
633 modelled $\delta^{18}O$ (green) and long-term groundwater $\delta^{18}O$ mean (pink). (D) Cl declines at Site
634 1a until Feb where it shows a slight increase until the drip becomes dry, while Site 2a shows
635 a steady increase until in July 2007 where it stabilizes for the remainder of the monitoring
636 period. (E) Post-fire response shows a decline in Mg at Site 1a until dry and a steady increase
637 at Site 2a until in Dec 2007 where it remains stable. (F) Site 1a shows step wise decline in Ca
638 at Site 1a until dry, while at Site 2a a very gradual increase until June 2007 is seen while the
639 remainder of the monitoring period remains steady. (G) Response for Sr shows Site 1a
640 declining and Site 2a peaking in Dec 2007; an identical response to Mg and at both sites. (H)
641 K post-fire at Site 1a shows high concentrations, double that of Site 2a but stable, while at
642 Site 2a shows a very gradual increase but is relatively stable over time. (I) SO_4 at Site 1a
643 remains stable until 2007 where it increases until dry and at Site 2a it shows a steady
644 increasing trend. Site 1a has double the initial absolute concentration in comparison to Site
645 2a, similar to other solutes.

646

Hydrol. Earth Syst. Sci. Discuss., doi:10.5194/hess-2016-1, 2016
Manuscript under review for journal Hydrol. Earth Syst. Sci.
Published: 19 January 2016

647

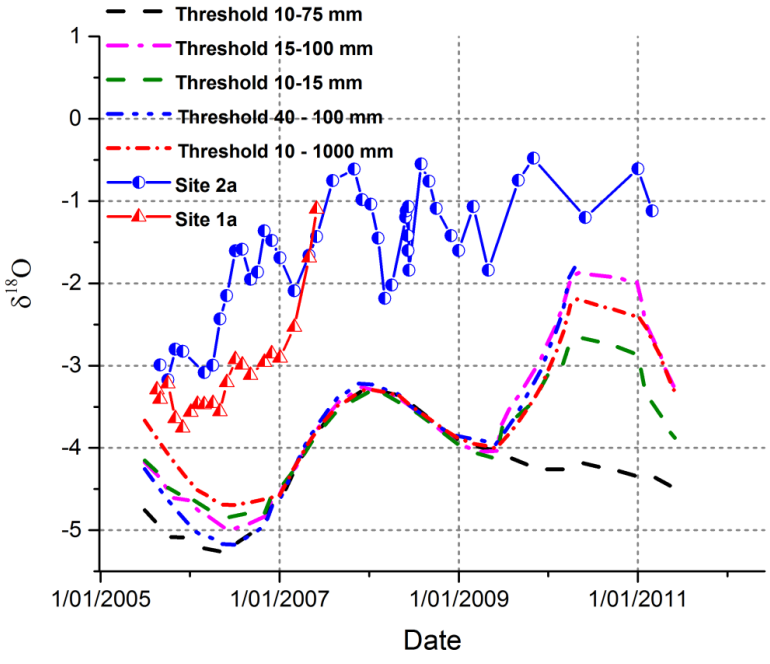

648

649 Figure 4. Shows outputs under varying thresholds in our forward model (model from Baker et
650 al., 2010) which accounts for climatic and various epikarst threshold values that control
651 isotopic values. Given no output matches observed dripwater composition we can infer that a
652 localised factor has influenced isotopic compositions

Hydrol. Earth Syst. Sci. Discuss., doi:10.5194/hess-2016-1, 2016
Manuscript under review for journal Hydrol. Earth Syst. Sci.
Published: 19 January 2016

Hydrology and Earth System Sciences
Discussions

653

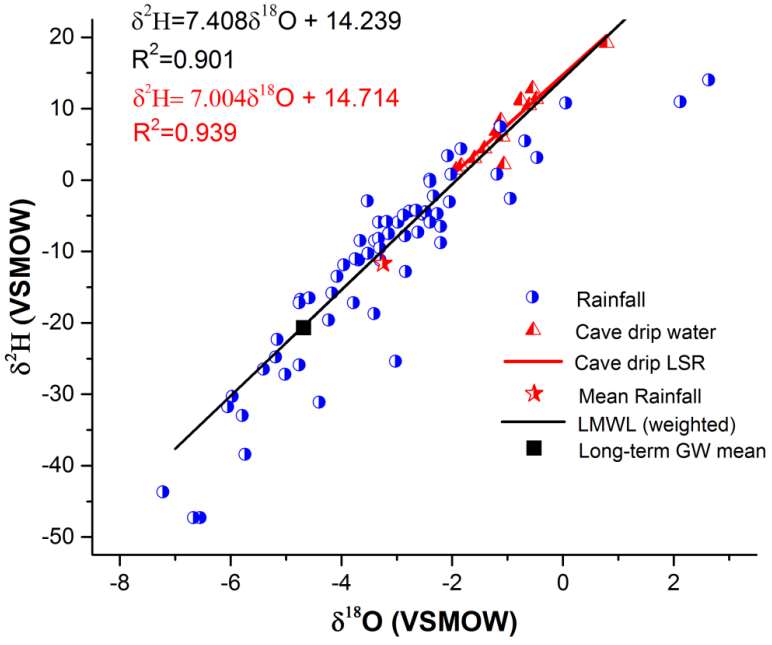

654

655 Figure 5. Shows compositions of δ^2H against $\delta^{18}O$ of our rainfall data (blue) during the
656 monitoring period (ANSTO, unpublished), cave dripwater (red), long-term local groundwater
657 mean (black) (0 – 10 ka, n=43, Southern Perth Basin from Turner and Thorpe, (2001)), and
658 rainfall mean (red). A least squares regression (LSR) is plotted for cave dripwater (red line)
659 and falls close to the local meteoric water line (LMWL, black) which is calculated using a
660 weighted least squares regression (WLSR) using Hughes and Crawford, (2011).

661

Hydrol. Earth Syst. Sci. Discuss., doi:10.5194/hess-2016-1, 2016
Manuscript under review for journal Hydrol. Earth Syst. Sci.
Published: 19 January 2016

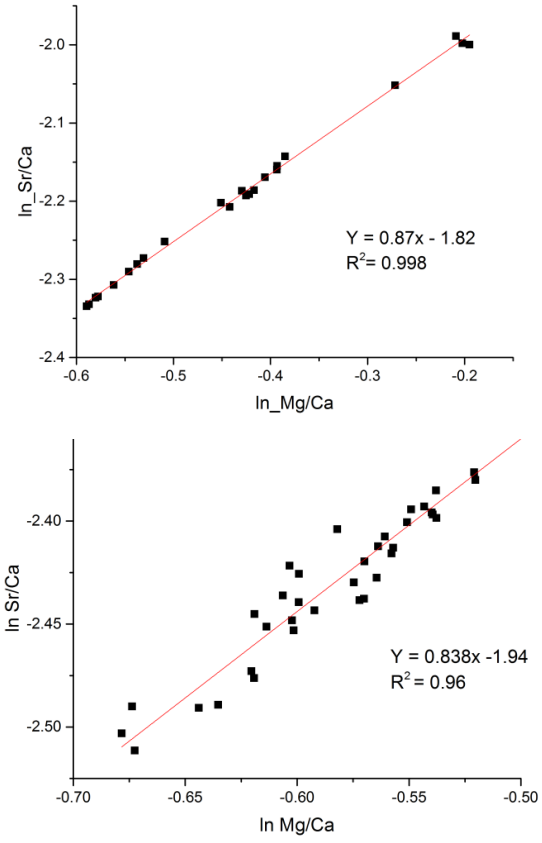

Figure 6. Shows ln_Sr/Ca vs. ln_Mg/Ca using the method described in Sinclair, (2011) at Site 1a (A) and Site 2a (B) to determine if PCP is occurring. Both sites fall within the diagnostic model for water-rock interactions that include PCP by Sinclair (2011) and Treble et al. (2015) who found PCP to be a dominating in-cave process in Golgotha Cave 300 km, south of Yonderup Cave. Thus a number of processes may be responsible for causing heterogeneity in Ca concentrations.

Hydrol. Earth Syst. Sci. Discuss., doi:10.5194/hess-2016-1, 2016
Manuscript under review for journal Hydrol. Earth Syst. Sci.
Published: 19 January 2016

Hydrology and Earth System Sciences
Discussions

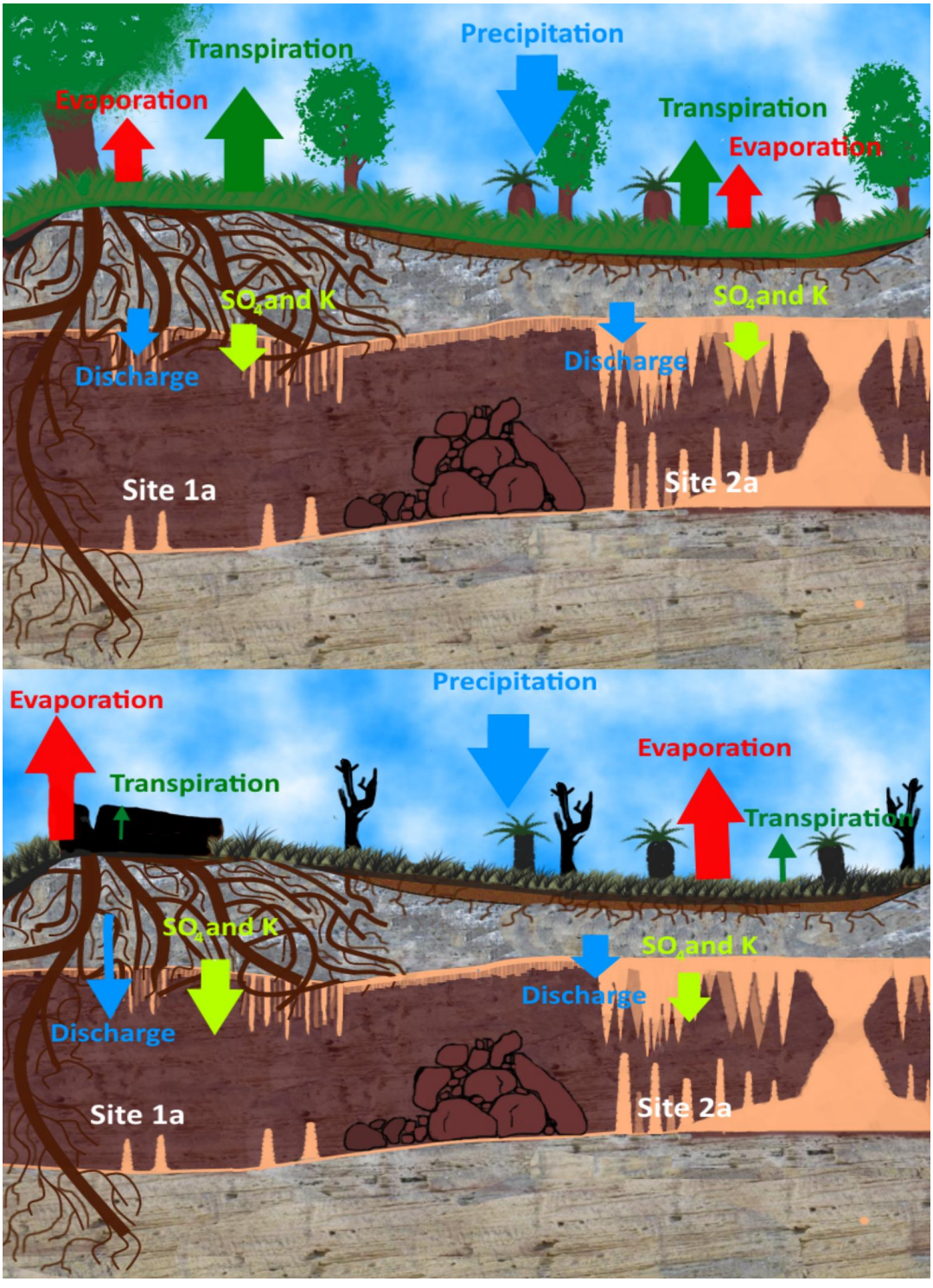

680

Hydrol. Earth Syst. Sci. Discuss., doi:10.5194/hess-2016-1, 2016
Manuscript under review for journal Hydrol. Earth Syst. Sci.
Published: 19 January 2016

Figure 7) Evaporation (red) increases post-fire at both sites due to a reduction in albedo and vegetation cover while precipitation (blue) remains the same and initial transpiration (green) decreases, but recovers over time. Site 2a shows higher $\delta^{18}O$ and an increase in concentrations of solutes including SO_4 and K (lime) due to evaporation and slow increase in transpiration due to vegetation recovery, with cumulative water balance (CWB) remaining the same. While Site 1a shows higher $\delta^{18}O$ in response to evaporation and a decline in solute concentrations in response to increased discharge and a decrease in transpiration. However since SO_4 and K are from biomass-sourced ash increased discharge post fire at site 1a increases SO_4 and K in dripwater. Discharge increased immediately (blue) at this site but only lasted a few months post-fire. The drip became inactive one year after the fire an increase evaporation outweighed the reduction in transpiration (green), leading to depletion of the near-surface reservoir feeding Site 1a and an in active drip site.